TÜBİTAK

Turkish Journal of Biology

http://journals.tubitak.gov.tr/biology/

Research Article

Turk J Biol
(2013) 37: 620-628
© TÜBİTAK
doi:10.3906/biy-1301-81

The effect of sooty mold on fluorescence and gas exchange properties of olive tree

Sónia A.P. SANTOS[1,*], Conceição SANTOS[2], Sónia SILVA[2], Glória PINTO[2], Laura M. TORRES[3], António J.A. NOGUEIRA[2]

[1]Mountain Research Center (CIMO), School of Agriculture, Polytechnic Institute of Bragança, Campus de Santa Apolónia, Bragança, Portugal

[2]Department of Biology and Centre for Environmental and Marine Studies (CESAM), University of Aveiro, Aveiro, Portugal

[3]Centre for the Research and Technology of Agro-Environment and Biological Sciences (CITAB), Department of Agronomy, University of Trás-os-Montes and Alto Douro, Vila Real, Portugal

Received: 01.02.2013 • **Accepted:** 05.05.2013 • **Published Online:** 06.09.2013 • **Printed:** 04.10.2013

Abstract: Sooty mold is a complex of dark-pigmented fungi that covers leaves and branches of the olive tree (*Olea europaea* L.). This coverage can bring several consequences for the plant, such as decrease of the photosynthetic rate. Therefore, this study aims to understand the effect of sooty mold on fluorescence and gas exchange of olive leaves. Olive leaves were field-collected and histological, physiological (water content, fluorescence parameters, and carbon dioxide fluxes), and biochemical (osmolality; chlorophyll a, b, and a/b contents; and lipid peroxidation) analyses were performed in healthy leaves and in leaves covered with sooty mold. Histological analysis revealed a complex fungal hyphae proliferation on both leaf surfaces of covered leaves that predominated on the abaxial surface. Sooty mold-covered leaves showed significantly lower levels of water content and of basal (F_0), maximal (F_m), and variable fluorescence (F_v). The proliferation of the sooty mold resulted in a decrease of fluorescence parameters, foliar free gas exchanges, and water content. Based on these results, we can conclude that sooty mold infection could affect light reaching leaves and the normal physiological metabolism of the plant (as photosynthesis) would be affected, with consequences for production.

Key words: Sooty mold, *Olea europaea*, fluorescence, chlorophyll, gas exchange, CO_2 flux, histology, lipid peroxidation

1. Introduction

The cultivation of *Olea europaea* L. is a traditional part of European agriculture and has both socioeconomic and environmental importance, in particular in the Mediterranean Basin (Loumou and Giourga, 2003; Nuberg and Yunusa, 2003, Demiral et al., 2011). Despite its importance, olive faces several diseases that have a severe impact on tree production, one of which is sooty mold. It is accepted that sooty mold is a complex of dark-pigmented fungi of several genera (e.g., *Capnodium*, *Cladosporium*, and *Fumago*), which have been described as nonparasitic, saprophytic, and superficial on plants (Panis, 1977a; Reynolds, 1999; Jouraeva et al., 2006). This fungal complex covers both leaf surfaces and small branches, giving a black aspect to the olive tree (Reynolds, 1999).

The development of sooty mold in olive trees is typically a consequence of heavy infestations caused by black scale, *Saissetia oleae* (Olivier) (Hemiptera: Coccidae), a parthenogenetic insect pest that sucks plant sap. Much of the water and sugars in the sap pass through the black scale gut, being excreted and producing abundant honeydew that covers the olive leaves and supports the proliferation of the sooty mold (Passos-Carvalho et al., 2003; Jouraeva et al., 2006). Strategies to control this disease are still mostly restricted to spraying the olive tree with copper or pruning the trees, which reduces the population of *S. oleae* (e.g., Passos-Carvalho et al., 2003). Attempts to use *Fusarium larvarum* in the biocontrol of black scale proliferation have been proposed (Cozzi et al., 2002), though reliable transfer of this strategy to large-scale field trials is still needed.

The coverage of the leaves by the sooty mold complex can have several consequences for the olive tree. It has been proposed that one of the main problems associated with fungal leaf coverage is the decrease of photosynthesis, and thus a consequent alteration of the normal metabolism and physiology of the plant and ultimately of its growth. For example, Panis (1977b) and Passos-Carvalho et al. (2003) mentioned the negative effects of sooty mold on parameters such as photosynthesis, chlorophyll, and respiration of the olive tree, but no measurable evidence was provided. Studies on other species also showed the interference of sooty mold on leaf performance and

* Correspondence: saps@ipb.pt

photosynthesis (Wood et al., 1988; Sparks et al., 1991). Nevertheless, and despite the great economic importance of olive in Mediterranean countries, few studies have been done showing scientific data on sooty mold's effects on olive tree photosynthesis, gas exchanges, and leaf anatomy.

Plant responses to biotic stress can be assessed using several indicators, such as water content/osmolality; lipid peroxidation, such as malondialdehyde (MDA) production, which often presents good correlation with lipid membrane peroxidation; chlorophyll contents and fluorescence; and carbon dioxide flux (Shtienberg, 1992; Guo et al., 2005; Santos et al., 2005; Synková et al., 2006).

Understanding if the fungus has an effect on photosynthesis gives further knowledge on the interactions between host and fungus and contributes to the development of alternative strategies to control its proliferation. Therefore, the objective of this work was to study the effect of sooty mold on gas exchanges and related processes in covered olive leaves, in particular photosynthesis, by analyzing related photosynthetic parameters (chlorophyll content and fluorescence) and the enrichment or depletion of atmospheric CO_2. These quantitative data were complemented by histoanatomical analyses in healthy and in covered leaves.

2. Materials and methods

2.1. Plant material

In November 2006, 10 randomly selected olive trees of the Cobrançosa cultivar were sampled in an olive grove located in Paradela (Mirandela, in the northeast of Portugal, 41°32′38″N, 7°7′29″W). In each tree, 5 current-season branch segments with visible sooty mold coverage and 5 healthy branch segments were detached from the south-facing canopy at about the same elevation (2.0 m). Branches were taken to a growth chamber at 22 ± 2 °C, placed in a container with water, and left overnight to avoid dehydration.

2.2. Histological analysis

For light microscopy analysis, leaf samples were treated according to the method of Pinto (2007). Briefly, leaves with and without sooty mold were fixed in 2.5% glutaraldehyde in 1.25% (w/v) piperazine-N,N'-bis(2-ethane sulfonic acid) (PIPES) buffer (pH 7.4) for 3 h and washed in PIPES. Tissues were transferred to 1.0% (w/v) osmium tetroxide in PIPES buffer, rinsed, dehydrated through a graded ethanol series, and embedded in a graded low-viscosity epoxy resin. Semithin sections were stained with toluidine blue. Samples were analyzed in a Nikon Eclipse 80i light microscope (Nikon Corporation Nikon Instech Co., Kanagawa, Japan). For scanning electron microscopy (SEM) analysis, material preparation was performed according to Pinto et al. (2002). Briefly, leaf samples were fixed with 2.0% (v/v) glutaraldehyde in PIPES buffer. Dehydration was achieved by successive immersions in aqueous ethanol solutions of increasing concentration (30%–100% v/v), in acetone solutions of increasing concentration (30%–100% v/v), and finally in a critical point device (Bal-tec CPD 030, Liechtenstein) using CO_2 as transition agent. Samples were fixed on steel supports and coated with gold using a JEOL metallizer (FFC-1100, Japan) at 1100–1200 V, 5 mA. Samples were observed with a scanning electron microscope (Hitachi S-4100, Tokyo, Japan) at 20 kV.

2.3. Physiological parameters

2.3.1. Leaf water content

Water content was determined in 50 leaves covered with sooty mold and 50 healthy leaves. Fresh weight (FW) was obtained from leaves after field collection, and dry weight was obtained after drying leaves in the oven for 48 h at 60 °C. Water content was calculated using Eq. (1), as follows:

$$[(FW - DW) / FW] \times 100. \quad (1)$$

2.3.2. Fluorescence parameters

Chlorophyll fluorescence was monitored using a Plant Efficiency Analyzer (Hansatech Instruments, Norfolk, UK). Prior to measurement, 50 healthy leaves and 50 leaves covered with sooty mold were dark-adapted for 30 min and illuminated with a peak wavelength of 650 nm and a saturating light intensity of 3000 μmol m^{-2} s^{-1}. The maximum quantum yield of PSII $[(F_m - F_0) / F_m]$ was determined after the estimation of the basal nonvariable chlorophyll fluorescence (F_0) and the maximal fluorescence induction (F_m) with all PSII reaction centers open (Maxwell and Johnson, 2000).

2.3.3. CO_2 exchanges

The effect of sooty mold on leaf CO_2 fluxes was measured using an infrared CO_2 gas analyzer, model ADC 225-MK3 (Analytical Development Co., Ltd., Hoddesdon, UK), coupled to a thermal flow meter and using air collected outside the lab as reference air (Heinemeyer et al., 1989). This apparatus has 12 independent lines passing through sample holding chambers and 1 reference line. One olive branch segment with 8 leaves attached was introduced into each sample tube and CO_2 was measured during a period of 14 h at 20 °C. Six of the tubes contained branch segments with healthy leaves and the other 6 tubes contained branch segments with leaves with sooty mold. Furthermore, half of the tubes with healthy leaves were placed in the dark and the others were illuminated with a light intensity of 2000 lx (200 μmol m^{-2} s^{-1}). The same procedure was done with the sooty-mold leaves. A flow rate of 205 ± 10 mL min^{-1} (mean ± standard error of the mean) was maintained in both reference and sample tubes throughout the experiment. The CO_2 measurements were given by the differential between the CO_2 concentrations of the

air, leaving the sample compared to that of the reference. Based on preliminary experiments, 7 independent trials were used to generate a suitable number of replicates. In each trial, treatments were randomly assigned to each channel. After the measurements, the total leaf area of each sample, healthy area (HA), and covered area with sooty mold (CA) were quantified using the image analysis software SigmaScan Pro 5.0 (SPSS, 1999).

2.4. Biochemical parameters

2.4.1. Osmolality

Fifty leaves covered with sooty mold and 50 healthy leaves were submitted to freeze/unfreeze cycles to assure membrane rupture and centrifuged at 13,000 × *g* for 10 min (Santos et al., 2001). The osmolality of the leaf extracts was measured in an automatic osmometer (Knawer, Berlin, Germany) and expressed in mmol kg^{-1}.

2.4.2. Chlorophyll concentration

The concentrations of chlorophyll (chl) a, b, and a + b (chl T) and the a/b ratio were determined according to Arnon (1949) in the same 50 covered and healthy leaves used for the fluorescence measurements, after as much sooty mold as possible was removed from leaf surfaces by gently washing each infected leaf with tap water. The petioles and central veins were also removed from the leaves.

2.4.3. Estimation of lipid peroxidation

MDA level is routinely used as an index of lipid peroxidation and was estimated according to the method of Dhindsa and Matowe (1981). Sooty mold was removed from leaf surfaces by gently washing each infected leaf with tap water. For measurements, 0.25 g of fresh leaves was deep-frozen in liquid nitrogen and ground in 5 mL of 0.1% trichloroacetic acid (TCA) from a total of 50 samples of leaves covered with sooty mold and 50 samples of healthy leaves. After centrifuging at 10,000 × *g* for 10 min, 1 mL of extract was taken and 4 mL of TCA (20%) with thiobarbituric acid (TBA, 0.5%) was added. The mixture was heated for 30 min at 95 °C, immediately cooled in an ice bath, and centrifuged again at 10,000 × *g* for 10 min. The specific absorbance of products and nonspecific background absorbance were read at 532 and 600 nm, respectively. The concentration of MDA was determined in its unit equivalent using a molar extinction coefficient of 155 mM^{-1} cm^{-1} and was expressed as nmol g^{-1} fresh weight.

2.5. Data analysis

Principal component analysis (PCA) was applied to the results of biochemical parameters. PCA was chosen due to the expected linear response model relating biochemical parameters and the presence of sooty mold in leaves (Van den Brink et al., 2003). The analysis was performed with CANOCO for Windows, version 4.5 (ter Braak and Šmilauer, 2002), using fluorescence and biochemical parameters to play the role of species data, and a binary matrix with healthy and sooty mold-covered leaves was used to play the role of supplementary environmental data. Species data were centered and standardized within CANOCO for Windows. Biochemical parameters, except for CO_2 flux measurements, were compared using one-way ANOVA.

A model was developed to describe changes in ΔCO_2 that were assumed as reflecting the CO_2 exchanges associated with 3 different physiological processes: leaf respiration (LR), sooty mold respiration (SMR), and leaf photosynthesis (LP). The underlying assumptions concerning CO_2 exchanges were:

- Leaf respiration is assumed to be proportional to the noncovered area, since sooty mold may interfere with stomata gas exchanges in covered leaf areas;
- Sooty mold respiration is proportional to the covered area;
- Sooty mold blocks light absorption, not allowing the mesophyll to perform photosynthetic light-dependent reactions in covered leaf areas;
- Total covered area (CA) is correlated with both covered abaxial and adaxial areas.

Thus, the equations to represent each of these processes (LR, SMR, and LP) can be written as linear functions of the healthy area (HA) and covered area (CA):

$$LR = a + b \times HA, \quad (2)$$

$$SMR = c + d \times CA, \quad (3)$$

$$LP = e + f \times HA, \quad (4)$$

where *a, c*, and *e* are elevation constants and *b, d*, and *f* are slopes. The arguments supporting these assumptions will be further explained in Section 4.

Generically, ΔCO_2 can be written as

$$\Delta CO_2 = LR + SMR + LP, \quad (5)$$

where positive changes in ΔCO_2 are assumed to be associated with leaf respiration and with sooty mold respiration, and negative changes in ΔCO_2 are assumed to be associated with leaf photosynthesis. Some partial function can be equal to 0, depending on the existing conditions (light and extent of leaf coverage by sooty mold):

- Healthy leaves exposed to light:
  $\Delta CO_2 = LR + LP$ (6)
- Covered leaves exposed to light:
  $\Delta CO_2 = LR + SMR + LP$ (7)
- Healthy leaves in the dark:
  $\Delta CO_2 = LR$ (8)
- Covered leaves in the dark:
  $\Delta CO_2 = LR + SMR$ (9)

Eq. (5) and its coefficients were solved iteratively using the SOLVER add-in for Microsoft Excel 11 using the minimization of the residual sum of squares as the target. The goodness of fit of the regression model was assessed using the adjusted coefficient of determination (r^2_{adj}). The F-statistics for the regression were determined using standard methodologies (Zar, 1996).

Monte Carlo simulation was used to predict 95% confidence and prediction limits for the relationships established between predicted and measured changes in CO_2.

The relationships between the total covered area, the covered abaxial area (CAA_b), and the covered adaxial area (CAA_d) were established using linear regression. The slopes and elevations of the resulting equations were compared by ANCOVA (Zar, 1996). The significance level used for all analyses was always 0.05.

3. Results

Leaves with sooty mold showed a typical dark color covering large areas of both abaxial and adaxial surfaces, contrasting with the bright green color of healthy leaves (Figure 1A). Healthy leaves showed thick, waxy cuticle (mostly on the upper surface) and an abundant trichome complex, mostly on the abaxial surface, that often presented sunken stomata (Figure 1B). On the adaxial surface, the mesophyll had 3–4 layers overall of palisade parenchyma, while a larger number of spongy layers were present; besides the main vascular strand (with secondary growth), minor small vascular strands were also present in the leaf blade, independent of the presence of fungus (Figure 1C). In covered leaves, the presence of sooty mold hyphae was visible, mostly on the abaxial surface (Figure 1D and 1F). Often the presence of black scale was also

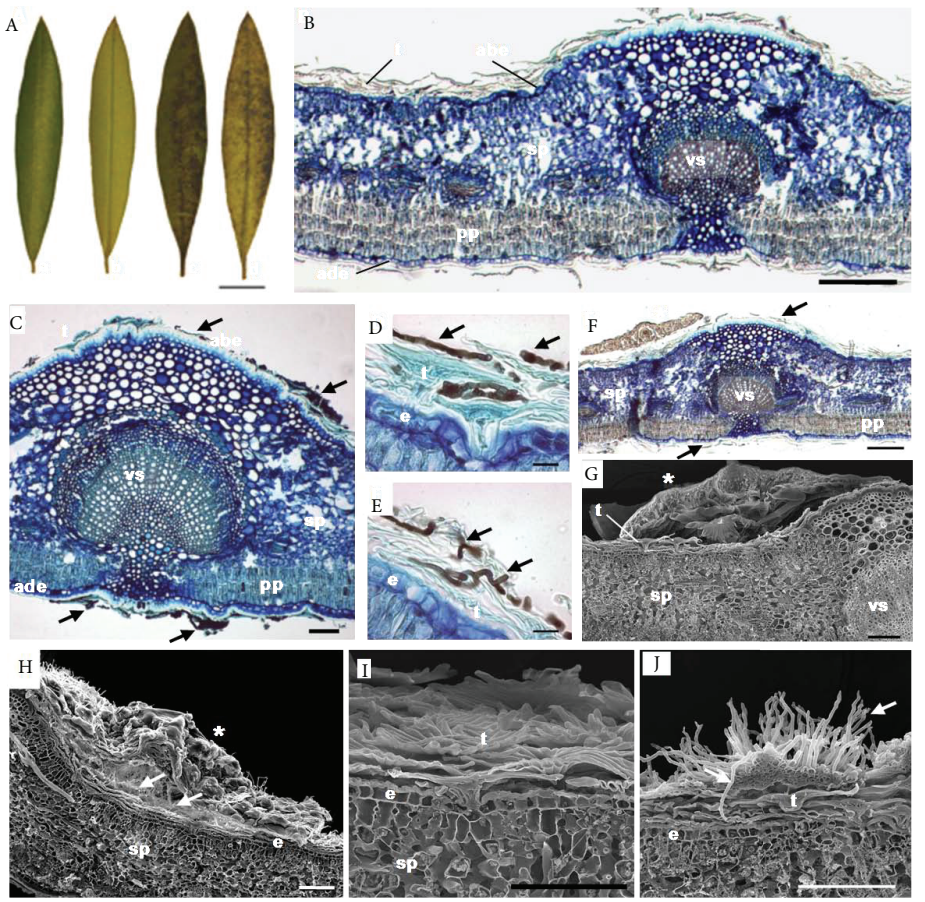

Figure 1. Comparative analysis of healthy leaves and sooty mold-covered leaves of *O. europaea*. A) Aspect of: a- adaxial surface of a healthy leaf; b- abaxial surface of a healthy leaf; c- adaxial surface of a covered leaf; d- abaxial surface of a covered leaf (scale bar = 1 cm). B) Light microphotograph of a healthy leaf cross-section (scale bar = 50 µm). C) Light microphotograph of a covered leaf cross-section (scale bar = 50 µm). D) and E) Details of sooty mold hyphae on leaf trichomes (scale bar = 50 µm). F) Light microphotograph of a covered leaf cross-section, where the black scale appears on the abaxial surface (scale bar = 50 µm). G) and H) SEM image of covered leaf cross-section with black scale on the abaxial surface (scale bars = 100 µm). I) SEM image of a healthy leaf cross-section (scale bar = 100 µm). J) SEM image of sooty mold hyphae on leaf trichomes (scale bars = 100 µm). Abbreviations: abe, abaxial epidermis; ade, adaxial epidermis; e, epidermis; pp, palisade parenchyma; sp, spongy parenchyma; t, trichome; vs, vascular strands. Arrows indicate the infection of sooty mold hyphae and asterisks show the transverse section of the black scale.

visible (Figure 1G and 1H). Both surfaces on covered leaves showed particular dark structures and hyphae proliferation covering the trichome complex (Figure 1J), and large air spaces were present between this dark and compact film (formed by the matrix–fungus–trichome mesh) and the leaf epidermis. Considering the inner leaf anatomy, no significant changes were observed between the mesophyll of covered and healthy leaves.

Healthy leaves had an average water content of 43.08 ± 0.40% (mean ± standard error of the mean) and an osmolality of 958.38 ± 35.30 mmol/kg. Sooty mold-covered leaves showed a significant decrease of water content to 38.96 ± 0.15%, but no differences in the osmolality were found (Table).

The average values of chl contents of healthy leaves showed that the content of chl b was less than half the content of chl a, and that chl a and b contents, as well as the chl a/b ratio, were not statistically affected ($P > 0.05$) by the presence of the sooty mold. Concerning chlorophyll fluorescence, the leaves covered with sooty mold showed statistically significant lower levels of basal (F_0), maximal (F_m), and variable fluorescence (F_v), but for maximal photochemical efficiency of PSII (given by F_v/F_m), no significant differences were found between healthy and sooty mold-covered leaves, and a mean value of 0.8 was determined (Table).

The ordination diagram resulting from the PCA analysis for different biochemical parameters is shown in Figure 2. In general, samples corresponding to leaves covered with sooty mold were clearly separated from those samples determined from healthy leaves. The most determinant parameters for PCA distribution were those

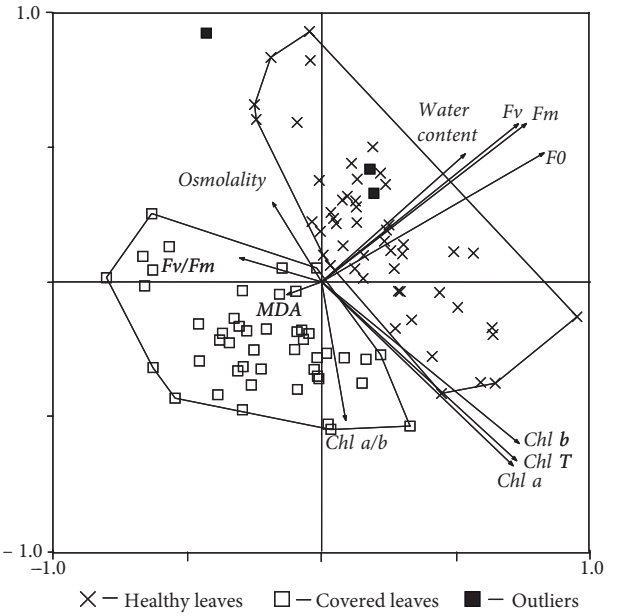

Figure 2. PCA ordination diagram for the different biochemical parameters measured in healthy and in sooty mold covered leaves. The first and second axis of PCA explained 34.6% and 25.3% of the total variability, respectively.

related with fluorescence (namely, F_0, F_m, and F_v) and water content, which were significantly higher in healthy leaves.

The differentials of CO_2 concentrations measured during a period of 14 h are shown in Figure 3. The main differences were observed between illuminated segment branches, where higher differentials of CO_2 concentrations were measured in sooty mold-covered leaves than in

Table. Mean ± standard error of the mean of each biochemical parameter determined in healthy leaves and in leaves covered with sooty mold and statistical output for ANOVA, n = 50.

Biochemical parameters	Healthy leaves	Covered leaves	Statistical output	
F_0	550.26 ± 9.50	291.20 ± 17.72	$F_{1, 80} = 57.67$	($P < 0.001$)
F_m	2874.80 ± 50.06	1608.70 ± 96 08	$F_{1, 80} = 64.00$	($P < 0.001$)
F_v	2344.96 ± 53.34	1317.90 ± 80.64	$F_{1, 80} = 59.51$	($P < 0.001$)
F_v/F_m	0.81 ± 0.00	0.82 ± 0.01	$F_{1, 80} = 2.08$	($P = 0.166$)
Osmolality (mmol/kg)	958.38 ± 35.30	969.38 ± 40 28	$F_{1, 80} = 0.15$	($P = 0.706$)
Chl a (mg/g FW)	0.99 ± 0.06	0.95 ± 0.05	$F_{1, 80} = 0.06$	($P = 0.808$)
Chl b (mg/g FW)	0.40 ± 0.03	0.36 ± 0.02	$F_{1, 80} = 0.37$	($P = 0.548$)
Chl a/b	2.46 ± 0.04	2.62 ± 0.04	$F_{1, 80} = 2.91$	($P = 0.105$)
MDA (nmol/g FW)	3.94 ± 0.10	4.15 ± 0.15	$F_{1, 80} = 1.62$	($P = 0.219$)
Water content (%)	43.08 ± 0.40	38.96 ± 0.15	$F_{1, 80} = 91.92$	($P < 0.001$)

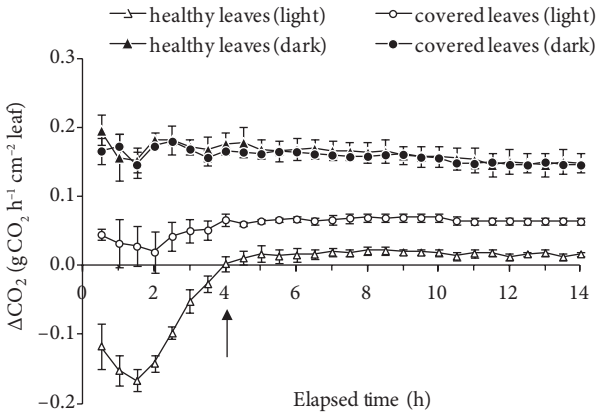

Figure 3. Differential concentrations of CO_2 (mean ± standard error, n = 21) measured during a period of 14 h in branch segments with healthy leaves and with sooty mold-covered leaves placed in the dark or in the light. Arrow indicates the compensation point.

healthy leaves. During the first 4 h of the experiment, negative values for differential of CO_2 concentrations were measured in illuminated healthy leaves. After this, the differential of CO_2 concentrations increased, reaching a value slightly above 0 that was maintained constantly until the end of the experiment. Illuminated sooty mold-covered leaves showed mean positive values during the considered period, although lower values were measured in the first 2 h of the experiment. Considering segment branches placed in darkness, the highest mean values for the differential of CO_2 concentrations were measured in covered leaves, although clear differences between sooty mold-covered leaves and healthy leaves were not apparent (Figure 3). The solution of Eq. (5), which describes the differential of CO_2 concentration, yielded the following results (where 3 observations were considered outliers and were eliminated):

$\Delta CO_2 = (1.850 + 0.041 \times HA) + (1.162 + 0.029 \times CA) - (1.819 + 0.039 \times HA)$ (light),

$\Delta CO_2 = (1.850 + 0.041 \times HA) + (1.162 + 0.029 \times CA)$ (dark),

with an $r^2_{adj} = 80.5\%$ (n = 81) and $F_{1, 79} = 67.2$, $P < 0.0001$. From these general equations we can extract partial equations associated with each of the experimental conditions tested in our experimental design.

- $\Delta CO_2 = (1.850 + 0.041 \times HA) - (1.819 + 0.039 \times HA)$, for healthy leaves exposed to light.
- $\Delta CO_2 = (1.850 + 0.041 \times HA) + (1.162 + 0.029 \times CA) - (1.819 + 0.039 \times HA)$, for covered leaves exposed to light.
- $\Delta CO_2 = (1.850 + 0.041 \times HA)$, for healthy leaves in the dark.
- $\Delta CO_2 = (1.850 + 0.041 \times HA) + (1.162 + 0.029 \times CA)$, for covered leaves in the dark.

The residuals were randomly distributed and were independent of both the variations of the healthy area of the leaves (HA) (Figure 4A) and of the covered area with sooty mold (CA) (Figure 4B).

As shown from the scatter plots of measured versus predicted values for the differential of CO_2 concentration, the fitted values compare well with those measured, indicating that the developed model provides a good description of the data (Figure 5).

In covered leaves, correlation analysis showed that the area of sooty mold on the adaxial surface did not correlate with the area on the abaxial surface ($r = 0.113$; $df = 40$, $P = 0.158$). However, strong correlations and dependencies were found between total covered area (CA) and:

- the covered abaxial area (CAA_b),
  $CA = 12.352 + 0.905\ CAA_b$ ($r = 0.732$; $df = 40$, $P < 0.001$); (10)
- the covered adaxial area (CAA_d),
  $CA = 17.696 + 0.868\ CAA_d$ ($r = 0.595$; $df = 40$, $P = 0.003$). (11)

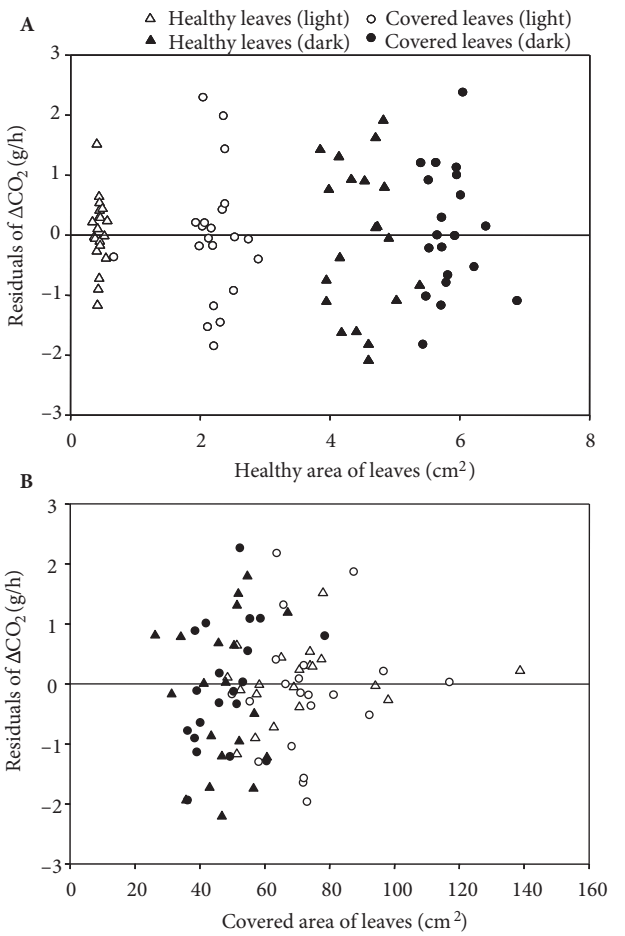

Figure 4. Relationship between the residuals from model predictions and each of the independent variables: A) healthy and B) covered area of the leaves.

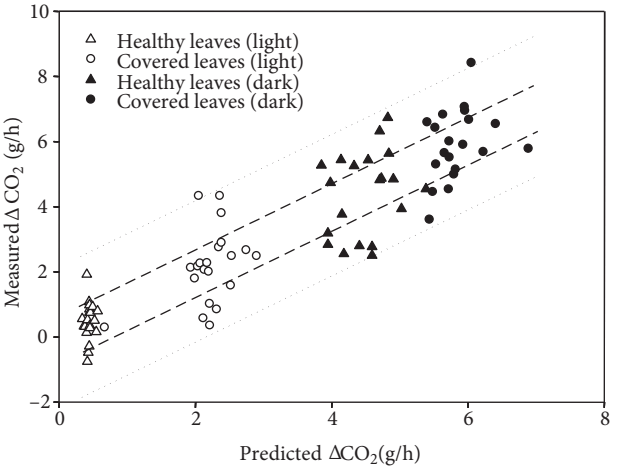

Figure 5. Relationship between predicted and measured changes in CO_2. Dashed lines express the trends in 95% confidence limits and dotted lines express the trends in the 95% prediction limits (these limits were calculated from Monte Carlo simulations).

These equations showed statistically identical slopes (ANCOVA: $F_{1, 80} = 0.028$; $P = 0.869$), but the elevations were statistically different (ANCOVA: $F_{1, 81} = 9.055$; $P = 0.0035$).

4. Discussion

Histological studies confirmed that olive trees are adapted to dry conditions by presenting, e.g., leaves with thick waxy cuticle on the adaxial surface and abundant hairs, sunken stomata, and small vessels on the abaxial surface. These characteristics have been described for other cultivars, too (e.g., Beede and Goldhamer, 1994; Nuberg and Yunusa, 2003). Histological data also confirmed that the fungal hyphae did not enter the mesophyll tissues and may form a dense and complex fungal matrix covering both sides of the leaves. Furthermore, no significant changes between the mesophyll anatomy of healthy and covered leaves were found. In addition, Nieves-Rivera (2005) reported that *Avicennia germinans* leaves covered with sooty mold could remain robust and intact. Similar studies on sooty mold in mahogany (*Swietenia macrophylla*) also showed no penetration in leaves and no histological changes inside the leaves (Filho and Paiva, 2006). The presence of this complex fungal matrix, in particular on the adaxial surface, limits the light reaching the mesophyll cells, as presumed by other authors (e.g., Panis 1977b; Passos-Carvalho et al., 2003). Filho and Paiva (2006) showed that sooty mold on the adaxial surface promoted a light blockage of more than 40% of light in mahogany leaves, with severe consequences to photochemical activity, while Wood et al. (1988) demonstrated that these fungal complexes block light mostly at wavelengths between 400 and 700 nm.

Besides the main effects on adaxial leaf surfaces, the distribution of the fungi on the abaxial surface may also affect stomata function and gas exchange. Histological analyses of covered olive leaves showed, in general, a higher distribution of the fungi on the abaxial surface with respect to the adaxial surface. These data strongly support the hypothesis that, by creating a microenvironment immediately outside the stomata (e.g., increasing the relative humidity), sooty mold regulates stomata functioning, affecting gas exchange (photosynthesis, respiration, and transpiration).

The water content decreased under sooty mold coverage conditions, indicating that plant–water relationships may be affected by this disease. In olive tree, sooty mold is strongly associated with black scale that in turn is associated with high temperatures (Noguera et al., 2003), and the negative effects of black scale and sooty mold cannot be separated. Decrease in the observed water content could also be explained by the water and sugars in the sap passing through the black scale gut. Considering the effects on chlorophyll, the data show that sooty mold does not significantly affect chl a and chl b contents.

Photochemical efficiency monitored by measuring chlorophyll fluorescence enabled the assessment of photosynthetic functioning in response to fungal infection. The decrease of F_0 found for covered leaves indicates that sooty mold directly or indirectly affects the PSII reaction centers. In addition, the reduction of F_m may reflect an increase of energy dissipation and/or indicate a reduction in the saturating light intensity reaching the mesophyll due to the presence of the fungal filter. This last hypothesis is the most likely as no significant changes were observed in the Fv/F_m ratio, indicating that the PSII photochemical efficiency was not apparently affected. Moreover, F_v/F_m values, which can be considered as a measure of the quantum efficiency of the electron transport in PSII (Maxwell and Johnson, 2000), were within the range of values of healthy plants (0.75–0.85) (Schreiber et al., 1994). Thus, the nondetected differences in chlorophylls may suggest that these pigments in the reaction centers may not be affected and that the thick black coverage of the leaf created by the sooty mold acts as a barrier that affects light reaching leaves. Nieves-Rivera (2005) also reported nonadverse effects of sooty mold on photosynthesis, Nevertheless, the light-harvesting complexes are also composed of other pigments (e.g., carotenoids), the contents of which should be analyzed in the future. The effect of sooty mold on oxidative stress is particularly important, but with the data reported it is impossible to correlate fungi and oxidative stress. However, further investigation should be implemented. The leaves analyzed are from the current season, and therefore the coverage process may be considered at an initial stage. Therefore, an analysis of the development with time of

sooty mold coverage would give valuable information on the interaction between sooty mold attack and oxidative stress, as well as chloroplast degradation and eventual leaf-induced senescence.

The model used in this paper showed with high reliability that light is a determinant factor in the analyses of CO_2 fluxes associated with sooty mold–leaf interactions. Thus, under light conditions, the net CO_2 flux measured in healthy leaves is due to respiration and photosynthesis (the combination of Eqs. (2) and (4) gives Eq. (6); see Section 2). In this case, a negative differential of CO_2 flux was measured during the first hours of the experiment in healthy leaves, demonstrating that in a short time period, photosynthesis occurred at higher rates than respiration, until a compensation point was reached, where photosynthesis plus respiration equals 0. After 4 h of the experiment, positive values for differential of CO_2 were measured, meaning that photosynthesis decreased, probably due to water limitations. On the other hand, in covered leaves, the net CO_2 flux is due to leaf and sooty mold respirations and leaf photosynthesis (the combination of Eqs. (2) to (4) gives Eq. (7)). Results showed positive values for differential CO_2 fluxes, even in the first hours of the experiment, supporting the idea that photosynthesis decreased and/or respiration increased.

Under dark conditions, in healthy leaves, only leaf respiration is considered (Eqs. (2) and (8)), while in covered leaves both leaf and sooty mold respirations are present (combination of Eqs. (2) and (3) gives Eq. (9)). Thus, covered leaves presented higher differential CO_2 fluxes than healthy leaves, reflecting the sum of leaf and fungal complex respirations. Olive is a hypostomatic species (e.g., Baldini et al., 1997; Chartzoulakis et al., 1999) and gas exchanges will only take place through the lower surface. Therefore, due to the microenvironments created by the fungal matrix, CO_2 exchanges would be affected by the coverage of the abaxial surface.

Based on the given identical slopes but on different elevations, Eqs. (10) and (11) strongly support the idea that the abaxial surface is more susceptible to the establishment of sooty mold, and once it occurs, it leads to higher areas of leaf coverage. This fact has never been properly described, but it is highly predictable due to both higher occurrence of the black scale on the abaxial surface (Pereira, 2004) and the characteristics of the lower surface (thinner cuticle, stomata, spongy parenchyma, and higher proximity of phloem cells) (e.g., Baldini et al., 1997).

In conclusion, this study showed that the coverage of the leaf by the sooty mold creates a shade effect that acts as a barrier that limits the light reaching leaves, mainly due to fungal coverage on the adaxial surface, and to free gas exchange, mainly due to fungal proliferation on the abaxial surface. The main outcome of this interference is that the normal physiological metabolism of the plant involving light absorption and CO_2 exchange would be severely affected. Furthermore, the adopted experimental design and the analytical framework outlined here have the potential to be further exploited in studies involving complex interactions between sooty mold and host species in general and olive trees in particular. The validity of this model at different stages of the disease progression should also be explored.

Acknowledgments

We thank the owners of the olive grove who permitted access for this study. This study was funded by Project AGRO 482: "Protecção contra pragas do olival numa óptica de defesa do ambiente e do consumidor".

References

Arnon DI (1946). Copper enzymes in isolated chloroplasts. Polyphenoloxidases in *Beta vulgaris*. Plant Physiol 24: 1–10.

Baldini E, Facini O, Nerozzi F, Rossi F, Rotondi A (1997). Leaf characteristics and optical properties of different woody species. Trees 12: 73–81.

Beede RH, Goldhamer DA (1994). Olive irrigation management. In: Ferguson L, Sibbett GS, Martin GC, editors. Olive Production Manual. Oakland, CA, USA: University of California Publication 3353, pp. 61–68.

Chartzoulakis K, Patakas A, Bosabalidis AM (1999). Changes in water relations, photosynthesis and leaf anatomy induced by intermittent drought in two olive cultivars. Environ Exp Bot 42: 113–120.

Cozzi G, Stornelli C, Moretti A, Logrieco A., Porcelli F (2002). Field evaluation of *Fusarium larvarum* formulations in the biocontrol of *Saissetia oleae* on olive in Apulia. Acta Hortic 586: 811–814.

Demiral MA, Aktaş Uygun D, Uygun M, Kasırğa E, Karagözler AA (2011). Biochemical response of *Olea europaea* cv. Gemlik to short-term salt stress. Turk J Biol 35: 433–442.

Dhindsa RS, Matowe W (1981). Drought tolerance in two mosses: correlated with enzymatic defense against lipid peroxidation. J Exp Bot 32: 79–91.

Filho JPL, Paiva EAS (2006). The effect of photosynthesis and mesophyll structure of Mahogany (*Swietenia macrophylla*) King., Meliaceae). Bragantia 65: 11–17.

Guo DP, Guo YP, Zhao JP, Liu H, Peng Y, Wang QM, Chen JS, Rao GZ (2005). Photosynthetic rate and chlorophyll fluorescence in leaves of stem mustard (*Brassica juncea* var. *tsatsai*) after turnip mosaic virus infection. Plant Sci 168: 57–63.

Heinemeyer O, Insam H, Kaiser EA, Walenzik G (1989). Soil microbial biomass and respiration measurements: an automated technique based on infra-red gas analysis. Plant Soil 116: 191–195.

Jouraeva VA, Johnson DL, Hassett JP, Nowak DJ, Shipunova NA, Barbarossa D (2006). Role of sooty mold fungi in accumulation of fine-particle-associated PAHs and metals on deciduous leaves. Environ Res 102: 272–282.

Loumou A, Giourga C (2003). Olive groves: "The life and identity of the Mediterranean". Agr Hum Values 20: 87–95.

Lutts S, Kinet JM, Bouharmont J (1996). NaCl-induced senescence in leaves of rice (*Oryza sativa* L.) cultivars differing in salinity resistance. Ann Bot 78: 389–398.

Maxwell K, Johnson GN (2000). Chlorophyll fluorescence – a practical guide. J Exp Bot 51: 659–668.

Nieves-Rivera AM (2005). Coastal Mycology of Puerto Rico: A Survey and Biological Aspects of Marine Estuarine and Mangrove Fungi. PhD, University of Puerto Rico, San Juan, Puerto Rico.

Noguera V, Verdú MJ, Gómez Cadenas A, Jacas JA (2003). Ciclo biológico, dinámica poblacional y enemigos naturales de *Saissetia oleae* Olivier (Homoptera: Coccidae), en olivares del Alto Palancia (Castellón). Bol San Veg Plagas 29: 495–504 (article in Spanish).

Nuberg I, Yunusa I (2003). Olive water use and yield - monitoring the relationship. A report for the Rural Industries Research and Development Corporation. Kingston, ACT, Australia: RIRDC.

Panis A (1977a). Lecaninos (Homoptera, Coccoidea, Coccidae) dentro del plan de lucha integrada en la citricultura mediterránea. Bol San Veg Plagas 3: 111–119 (article in Spanish).

Panis A (1977b). Observations sur la propagation et les consequences de la fumagine de l'olivier. Olea: 59–62 (article in Spanish).

Passos-Carvalho J, Torres LM, Pereira JA, Bento AA (2003). A cochonilha-negra *Saissetia oleae* (Olivier, 1791) (Homoptera: Coccidae). Lisbon, Portugal: INIA/UTAD/ESAB (in Portuguese).

Pereira JAC (2004). Bioecologia da cochonilha negra, *Saissetia oleae* (Olivier), na oliveira, em Trás-os-Montes. PhD, University of Trás-os Montes and Alto Douro, Vila Real, Portugal (in Portuguese).

Pinto G (2007). Regeneração de plantas de *Eucalyptus globulus* por embriogénese somática. PhD, University of Aveiro, Aveiro, Portugal (in Portuguese).

Pinto G, Valentim H, Costa A, Santos CV (2002). Somatic embryogenesis in leaf callus from mature *Quercus suber* L. tree. In Vitro Cell Dev Pl 38: 569–572.

Reynolds DR (1999). *Capnodium citri*: the sooty mold fungi comprising the taxon concept. Mycopathologia 148: 141–147.

Santos C, Fragoeiro S, Phillips A (2005). Physiological response of grapevine cultivars and a rootstock to infection with *Phaeoacremonium* and *Phaeomoniella* isolates: an in vitro approach using plants and calluses. Sci Hortic 103: 187–198.

Santos CV, Campos A, Azevedo H, Caldeira G (2001). Nutritional imbalance and senescence induced in plants and *calli* exposed to KCl. J Exp Bot 52: 351–360.

Schreiber U, Bilger W, Neubauer, C (1994). Chlorophyll fluorescence as a nonintrusive indicator for rapid assessment of in vivo photosynthesis. In: Schulze ED, Caldwell, MM, editors. Ecophysiology of Photosynthesis. Berlin: Springer, pp. 49–70.

Shtienberg D (1992). Effects of foliar diseases on gas exchange processes: a comparative study. Phytopathology 82: 760–765.

Sparks D, Yates IE (1999). Pecan cultivar susceptibility to sooty mold related to leaf surface morphology. J Am Soc Hort Sci 116: 6–9.

SPSS (1999). SigmaScan Pro 5.0.0 – Image Analysis Software. Chicago: SPSS Inc.

Synková H, Semorádová Š, Schnablová R, Müller K, Pospíšilová J, Ryšlavá H, Malbeck J, Čeřovská N (2006). Effects of biotic stress caused by *Potato virus Y* on photosynthesis in *ipt* transgenic and control *Nicotiana tabacum* L. Plant Sci 171: 607–616.

ter Braak CJF, Šmilauer P (2002). CANOCO Reference Manual and User's Guide to CANOCO for Windows: Software for Canonical Community Ordination, Version 4.5. Ithaca, NY, USA: Microcomputer Power.

Van den Brink PJ, Van den Brink NW, ter Braak CJF (2003). Multivariate analysis of ecotoxicological data using ordination: demonstrations of utility on the basis of various examples. Aust J Ecotox 9: 141–156.

Wood BW, Tedders WL, Reilly, CC (1988). Sooty mold fungus on pecan foliage suppresses light penetration on net photosynthesis. Hort Science 23: 851–853.

Zar JH (1996). Biostatistical Analysis, 4th ed. London, UK: Prentice Hall.